**RESEARCH**

**Open Access**

# Flow-dependent shear stress affects the biological properties of pericyte-like cells isolated from human dental pulp

Giulia Bertani[1†], Rosanna Di Tinco[1†], Laura Bertoni[1†], Giulia Orlandi[1], Alessandra Pisciotta[1], Roberto Rosa[2], Luca Rigamonti[3], Michele Signore[4], Jessika Bertacchini[1], Paola Sena[1], Sara De Biasi[5], Erica Villa[1†] and Gianluca Carnevale[1*†]

## Abstract

**Background**  Human dental pulp stem cells represent a mesenchymal stem cell niche localized in the perivascular area of dental pulp and are characterized by low immunogenicity and immunomodulatory/anti-inflammatory properties. Pericytes, mural cells surrounding the endothelium of small vessels, regulate numerous functions including vessel growth, stabilization and permeability. It is well established that pericytes have a tight cross talk with endothelial cells in neoangiogenesis and vessel stabilization, which are regulated by different factors, i.e., microenvironment and flow-dependent shear stress. The aim of this study was to evaluate the effects of a pulsatile unidirectional flow in the presence or not of an inflammatory microenvironment on the biological properties of pericyte-like cells isolated from human dental pulp (hDPSCs).

**Methods**  Human DPSCs were cultured under both static and dynamic conditions with or without pre-activated peripheral blood mononuclear cells (PBMCs). Pulsatile unidirectional flow shear stress was generated by using a specific peristaltic pump. The angiogenic potential and inflammatory properties of hDPSCs were evaluated through reverse phase protein microarrays (RPPA), confocal immunofluorescence and western blot analyses.

**Results**  Our data showed that hDPSCs expressed the typical endothelial markers, which were up-regulated after endothelial induction, and were able to form tube-like structures. RPPA analyses revealed that these properties were modulated when a pulsatile unidirectional flow shear stress was applied to hDPSCs. Stem cells also revealed a down-regulation of the immune-modulatory molecule PD-L1, in parallel with an up-regulation of the pro-inflammatory molecule NF-kB. Immune-modulatory properties of hDPSCs were also reduced after culture under flow-dependent shear stress and exposure to an inflammatory microenvironment. This evidence was strengthened by the detection of up-regulated levels of expression of pro-inflammatory cytokines in PBMCs.

**Conclusions**  In conclusion, the application of a pulsatile unidirectional flow shear stress induced a modulation of immunomodulatory/inflammatory properties of dental pulp pericyte-like cells.

---

†Giulia Bertani, Rosanna Di Tinco and Laura Bertoni equally contributed to the study

†Erica Villa, Gianluca Carnevale are senior co-authors

*Correspondence:
Gianluca Carnevale
gianluca.carnevale@unimore.it
Full list of author information is available at the end of the article

## Introduction

Pericytes, vascular mural cells, are embedded in the basement membrane of blood microvessels including capillaries, precapillary arterioles and post-capillary venules.

Their role consists in reinforcing vascular structure and regulating microvascular blood flow, although they do not only serve as scaffolding as conventionally thought, but communicate with endothelial cells by direct physical contact and paracrine signaling pathways [1]. Besides exerting a primary function in endothelial stabilization, they indeed contribute to angiogenesis by differentiating into endothelial cells and forming new tubes [2]. It is noteworthy that the biological behavior of pericytes relies on the control exerted by endothelial cells (ECs) through the activation of multiple pathways and the release of pro-angiogenic factors, such as platelet-derived growth factor B (PDGF-B) [3] and angiopoietin 1 (Ang-1)/angiopoietin 2 (Ang-2)/Tie2, which are critically involved in embryonic or pathological angiogenesis. Moreover, it is known that interactions between ECs and pericytes are affected not only by biochemical stimuli but also by mechanical/physical factors, including blood pressure and flow-dependent shear stress, which may influence their cross talk and cell functions as well [4, 5].

Indeed, flow-dependent shear stress (FSS) plays a pivotal role in different pathological conditions, including chronic liver diseases. FSS alterations might affect the interstitial microenvironment and resident cells biological behavior, leading to the inflammatory process and a pro-fibrotic transition. These changes may support each other. For instance, in hepatocellular carcinoma the evolution of fibrosis associated with unresolved hepatic inflammatory process and the inherent progressive alteration of the normal laminar flow into a much more turbulent flow could be a key event in starting the process of endothelial activation [6].

In order to better clarify the role of pericytes in FSS-induced pathological conditions, our study used a pericyte-like cell population isolated from human dental pulp. Human dental pulp pericyte-like cells are entrapped in the loose connective tissue and are located in the perivascular area within dental pulp and express the typical pericyte markers nestin, PDGFRβ, smooth muscle actin α (αSMA) and VEGF [7].

In light of their embryological origin, hDPSCs own peculiar stemness properties that confer them high proliferative rate, immunomodulatory properties and low immunogenicity [8] as well as the ability to achieve the commitment into different cell lineages in vitro [9–13].

hDPSCs have also been shown to support tissue regeneration/homeostasis in vivo, by exerting direct and/or paracrine mechanisms on host progenitor cells [9, 11, 12]. It has been demonstrated that hDPSCs co-cultured with pre-activated peripheral blood mononuclear cells (PBMCs) exert immunomodulatory/anti-inflammatory properties by activating immune-checkpoint, including PD1/PD-L1 and Fas/FasL pathways, and by modulating the expression of the cytokines mainly involved in inflammatory response [8, 13, 14].

As established in the literature, stem cell properties are regulated by intrinsic mechanisms and extrinsic cues that emanate from the surrounding microenvironment. Inflammation is one of them [15]. To this regard, understanding the cross talk between inflammation and stem cells has aroused a huge interest among the scientific community, since it might elucidate the mechanisms activated by stem cells to respond to tissue damage and how to shape them to preserve the tissue homeostasis.

Based on these premises, to better understand the role of pericyte-like cells isolated from dental pulp, our study aimed to evaluate how flow-dependent shear stress may affect the biological properties of pericyte-like cells isolated from human dental pulp (hDPSCs) to predict their potential role in physiological and pathophysiological conditions.

## Methods

### Human dental pulp stem cells (hDPSCs) isolation and culture

This study was carried out in compliance with the recommendations of Comitato Etico Provinciale–Azienda Ospedaliero-Universitaria di Modena (Modena, Italy), which provided the approval of the protocol [ref. number 3299/CE; 5 September 2017]. Dental pulp tissue was obtained, after routine dental extraction, from third molars of adult subjects ($n = 3$; 30–35 years) who gave their written informed consent according to the Declaration of Helsinki. Cell isolation from dental pulp was carried out as previously described [9].

Briefly, the dental pulp was harvested from the teeth and enzymatically digested by means of 3 mg/mL type I collagenase and 4 mg/mL dispase in α-MEM. After filtering with a 100 μm cell strainer, the cell suspension was resuspended in α-MEM supplemented with 10% heat-inactivated fetal bovine serum (FBS), 2 mM L-glutamine, 100 U/mL penicillin, 100 μg/mL streptomycin at 37 °C and 5% $CO_2$. Following cell expansion, hDPSCs

were immune-selected by magnetic activated cell sorting (MACS), using MACS® separation kit according to manufacturer's instructions. Mouse IgM anti-STRO-1 and rabbit IgG anti-c-Kit primary antibodies (Santa Cruz, Dallas, TX, USA) were used and revealed by the following magnetically labeled secondary antibodies: anti-mouse IgM and anti-rabbit IgG (Miltenyi Biotec, Bergisch Gladbach, Germany).

### Endothelial differentiation of hDPSCs

STRO-1[+]/c-Kit[+] hDPSCs were induced toward the endothelial differentiation according to established protocols present in the literature [16]. Briefly, hDPSCs were cultured for 3, 5 and 7 days, respectively, in cell culture dishes at a density of $3 \times 10^3$ cells/dishes in endothelial medium consisting in EGM-2 supplemented with 2% FBS, 0.4% hFGF-B, 0.04% hydrocortisone, 0.1% VEGF, 0.1% R3-IGF-1, 0.1% ascorbic acid, 0.1% hEGF, 0.1% GA-1000, 0.1% heparin (EGM-2 Endothelial Medium BulletKit, Lonza Group Ltd, Basel, Switzerland). In order to evaluate the ability of hDPSCs to form tubule-like structure, tube formation analysis was performed using Matrigel® Matrix (Corning, New York, NY, USA) solution according to manufacturers' instructions. Undifferentiated hDPSCs were used as controls. The endothelial tubule-like vascular network formation was observed after 5 h of incubation under an inverted microscope. Images were acquired with a Nikon inverted microscope.

Tube-like structures were counted per 15,000 μm$^2$ areas on 5 different fields from 5 different experiments.

### Human umbilical vein endothelial cells (HUVECs) culture

HUVECs (ATCC, USA) were incubated in Vascular Cell Basal Medium (ATCC, USA) supplemented with Endothelial Cell Growth Kit-VEGF (ATCC, USA) at 37 °C, 5% $CO_2$ humidified incubator. Culture medium was changed every 2–3 days. Cells were used as controls.

### Human dental pulp stem cells cultured under dynamic conditions

Immune-selected hDPSCs suspension was filled into the channel slide of Ibidi μ-slides I Luer (height 0.4 mm) chambers (Ibidi, Gräfelfing, Germany) and allowed to attach overnight in standard culture medium at 37 °C, 5% $CO_2$ humidified incubator. The experimental setup was carried out according to the manufacturer's instructions (Ibidi) and is summarized in Fig. 1. Briefly, after connecting the channel slide to the peristaltic pump (React 4 Life, Peristaltic Pump R100-1 J), a unidirectional pulsatile flow of 1.5 dyn/cm$^2$ was applied with a 90 min time span after minor changes to the protocols previously described [17, 18].

### Peripheral blood mononuclear cells (PBMCs) isolation

PBMCs were isolated from fresh venous blood taken from 5 healthy adult volunteers. PBMCs were isolated
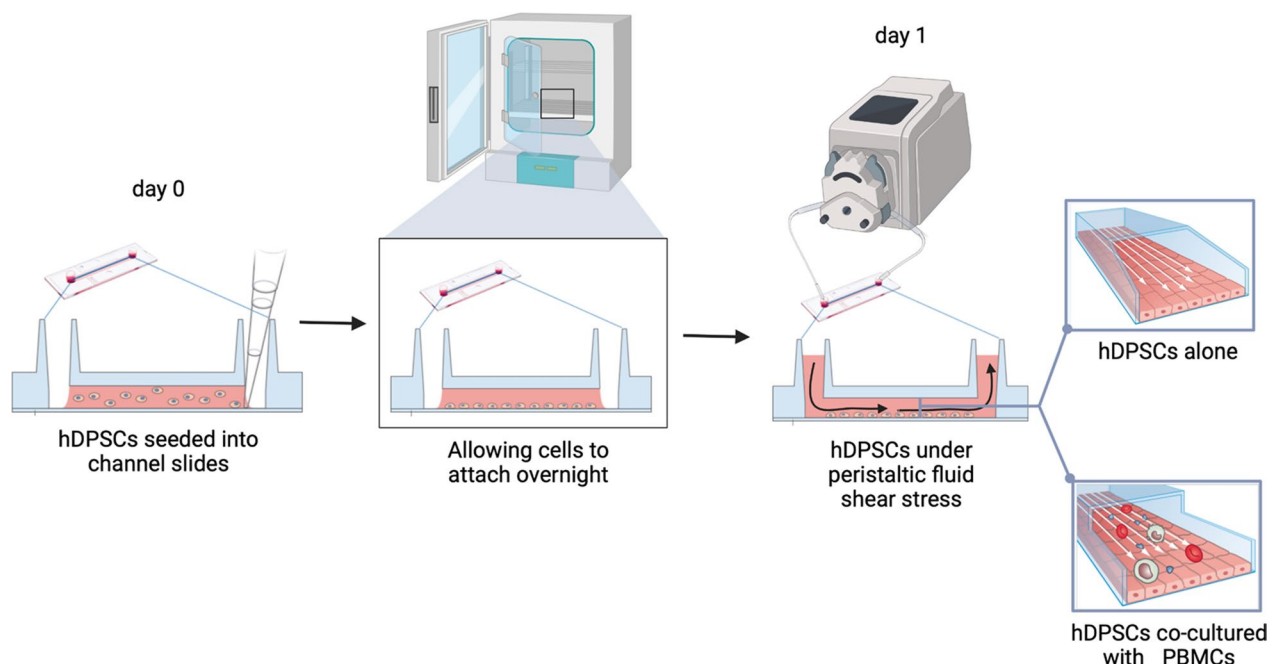


**Fig. 1** Experimental workflow of hDPSCs cultured under dynamic conditions. Illustrations were edited from Ibidi

Bertani *et al. Stem Cell Research & Therapy*     (2023) 14:31

Page 4 of 16

by using Histopaque (Sigma-Aldrich), according to the manufacturer' instructions and pre-activated as previously described [14]. In particular, direct co-culture system was established by seeding hDPSCs/PBMCs at a cell ratio 1:10 and cultured in RPMI 1640 medium supplemented with 10% FBS, 2 mM glutamine, 100 units/mL penicillin and 100 mg/mL streptomycin. Direct co-culture was performed both in static and dynamic conditions, respectively.

### Immunofluorescence and immunohistochemistry analyses
*Immunofluorescence.* Cells were fixed with 4% paraformaldehyde at 4 °C for 15 min and then permeabilized with 0.3% Triton X-100 for 5 min. After blocking with 3% bovine serum albumin (BSA) in pH 7.4 phosphate buffer saline (PBS) for 1 h, the cells were incubated at 4 °C overnight with the following primary antibodies: rabbit anti-PDGFR-β (Cell Signaling Technology, Trask Lane Danvers, MA, USA), rabbit anti-NG2 (Abcam), mouse anti-α smooth muscle actin (αSMA; Invitrogen), mouse anti-VEGF (Invitrogen, Waltham, MA, USA), rabbit anti-eNOS (Merck Millipore, Burlington, MA, USA), rabbit anti-ANGPT1 (GeneTex, California, USA), rabbit anti-Tie2 (Abcam, Cambridge, UK), mouse anti-STRO-1, rabbit anti-c-Kit (all diluted 1:100) Cell Signaling Technology, Trask Lane Danvers, MA, USA). Subsequently, the cells were incubated at 37 °C for 1 h at room temperature with the following secondary antibodies: goat anti-mouse Alexa488, goat anti-rabbit Alexa 546, goat anti-mouse Alexa546, goat anti-rabbit Alexa488 (all diluted 1:200; Thermo Fisher). Cell morphology was evaluated through immunolabeling with TRITC-conjugated, anti-phalloidin antibody (Abcam, Cambridge, UK).

Nuclei were counterstained with 1 μM 4,6-diamidino-2-phenylindole (DAPI) (Sigma-Aldrich). Images were captured by using Nikon A1 confocal laser scanning microscope as previously described [8].

*Immunohistochemistry.* Dental pulp samples were fixed in 4% paraformaldehyde in PBS and then paraffin-embedded. Five-micrometer-thick sections were cut, and immunohistochemistry carried out as previously described [9].

The following primary antibodies were used: mouse anti-VEGF (Invitrogen, Waltham, MA, USA) and rabbit anti-PDGFR-β (1:100, Cell Signaling Technology, Trask Lane Danvers, MA, USA). The sections were lightly counterstained with hematoxylin, mounted, and analyzed under an optical Nikon microscope.

### FACS analysis
In order to evaluate the expression of the typical mesenchymal stem cells (MSCs) markers, immune-selected hDPSCs, both in static and dynamic culture conditions, underwent FACS analysis against CD73, CD90, CD105, CD34, CD45, HLA-DR, as formerly described by Conserva et al. [19]. Following trypsin dissociation, cells were resuspended in culture medium and were stained with the following fluorochrome-conjugated antibodies (Abs): anti-human-CD73-PE-CY7, anti-human-CD90-FITC, anti-human-CD105-APC, anti-human-CD45-PE, and anti-human-HLADR-PE-CY7 (all from BD Biosciences, Franklin Lakes, NJ, USA); and anti-human-CD34-ECD (Beckman Coulter, Fullerton, CA, USA). A minimum of 10,000 cells per sample was acquired and analyzed by using the Attune Acoustic Focusing Flow Cytometer (Attune NxT, Thermo Fisher, Waltham, MA, USA). Data were analyzed by FlowJo 9.5.7 (Treestar, Inc., Ashland, OR, USA) under MacOS 10.

### Reverse phase protein microarray
For RPPA analysis, protein extracts were processed with a RIPA-like lysis buffer (LB) composed of TPER (Thermo Fisher Scientific, Waltham, MA, USA) and additioned with 300 mM NaCl and protease and phosphatase inhibitors cocktails (Merck Millipore, Burlington, MA, USA). Cell pellets were resuspended in an adequate volume of ice-cold LB, incubated on ice for 30 min and spun for 15 min at 12,000 rpm on a refrigerated centrifuge as previously described [20–22]. The protocols we used for RPPA analysis were previously optimized [20, 21]. Protein extracts were prepared by diluting 20 μg of protein extract with Novex™ Tris–Glycine SDS Sample Buffer 2X (Thermo Fisher Scientific, Waltham, MA, USA) as per the recipe by Laemmli [23]. Subsequently, RPPA samples were loaded onto an Aushon 2470 contact pin arrayer (Quanterix, MA, USA) and printed in technical triplicates onto nitrocellulose-coated slides (Grace Bio-Labs, OR, USA). The number of slides printed has been designed to include, but not limit the staining to at least 40 antibodies. In detail, a fraction of the printed slides was reserved for fluorescent detection of total protein content via Sypro Ruby (Thermo Fisher Scientific, Waltham, MA, USA) and the remaining slides were stored at − 20 °C for subsequent antibody staining. Immediately prior to staining, slides were treated with $1 \times$ ReBlot Mild Solution (Merck Millipore, Burlington, MA, USA) for 15 min, washed $2 \times 5$ min with PBS (Euroclone, Milan, Italy) and incubated for 2 h in a blocking solution containing 2% I-Block powder (Thermo Fisher Scientific, Waltham, MA, USA) and 0.1% Tween 20 in PBS. Immunostaining was carried out using a commercially available signal amplification kit (Agilent, CA, USA) based on catalyzed reporter deposition (CARD) [24]. Primary antibody binding was detected via secondary staining with biotinylated goat anti-rabbit IgG H + L (1:7500) (Vector Laboratories, CA, USA) or rabbit anti-mouse IgG (1:5000)

Bertani *et al. Stem Cell Research & Therapy*     (2023) 14:31

Page 5 of 16

(Agilent, CA, USA), followed by signal amplification and a tertiary streptavidin conjugated with IRDye680LT fluorophore (LI-COR Biosciences, NE, USA). Negative control slides were reserved on a per-staining run basis and incubated with secondary antibodies alone. Primary antibodies against the selected (phospho-)targets are part of a larger collection of antibodies that have undergone in-house validation for RPPA analysis using western blotting [25]. MicroVigene v5.2 (VigeneTech, Carlisle, MA) software was used for spot detection, local background subtraction, replicate averaging as well as for background amplification signal subtraction and total protein content normalization. Throughout the manuscript and in the figures, the above-described normalized RPPA data are referred to as normalized RPPA intensity or levels and are expressed in arbitrary units (A.U.). Raw RPPA data are reported in Additional file 1: Table S1.

### Western blot analysis

Where indicated, cell pellets were analyzed in western blot (WB). Whole cell lysates were obtained as formerly reported [10]. Briefly, 40 µg of protein extract per specimen was quantified by a Bradford Protein Assay (Bio-Rad), and then, SDS−polyacrylamide gel electrophoresis and subsequent protein transfer to nitrocellulose membranes were performed. The following antibodies were used: rabbit anti-PDGFR-β (Cell Signaling Technology, Trask Lane Danvers, MA, USA), rabbit anti-Tie2 (Abcam, Cambridge, UK), rabbit anti-eNOS (Merck Millipore, Burlington, MA, USA), rabbit anti-ANGPT1 (GeneTex California, USA), mouse anti-VEGF (Invitrogen, Waltham, MA, USA) and rabbit anti-cleaved caspase 3 (Cell Signaling Technology) diluted 1:1,000 in Tris-buffered saline (TBS) Tween 20 0.1%, plus 2% BSA and 3% non-fat milk and incubated overnight at 4 °C. Membranes were then incubated for 1 h at room temperature with HRP-conjugated anti-mouse and anti-rabbit secondary antibodies, diluted 1:2,000 in TBS Tween 20 0.1% plus 2% BSA and 3% non-fat milk. Membranes were then visualized by using Clarity Western ECL Substrate (Bio-Rad, Alfred Nobel Drive Hercules, CA, USA), according to the manufacturer's instructions. Anti-actin antibody was used as control of protein loading. Densitometry of PDGFR-β, Tie2, eNOS, ANGPT1, VEGF and cleaved caspase 3 was carried out with Fiji ImageJ software. An equal area was selected inside each band, and the mean of gray levels (in a 0–256 scale) was calculated. Data were then normalized to values of background and of control actin band [10].

### RNA purification and quantitative real-time PCR

Total RNA extraction was performed by using the PureLink™ RNA Micro Kit (Invitrogen, Waltham, MA, USA) according to manufacturer's instructions. RNA integrity and quantification were analyzed by a spectrophotometric method by using a NanoDrop 2000 device (Thermo Fisher Scientific, Waltham, MA, USA). Total RNA (1 µg) was reverse transcribed to cDNA using the QuantiTect Reverse Transcription Kit (Qiagen, Hilden, Germany), according to manufacturer's instructions. Levels of mRNA were quantitatively determined on a QuantStudio™ 3 Real-Time PCR System (Applied Biosystems, Thermo Fisher Scientific, Waltham, MA, USA) using the QuantiFast SYBR Green PCR Kit according to the manufacturer's instructions (Qiagen, Hilden, Germany). PCR primer sequences were as follows: hIL-2 (F: AAA GAAAACACAGCTACAACTGG, R: GAAGATGTT TCAGTTCTGTGGC); hIFNγ (F: GCATCGTTTTGG GTTCTCTTG R: AGTTCCATTATCCGCTACATCTG), hTNFα (F: ACTTTGGAGTGATCGGCC, R: GCTTGA GGGTTTGCTACAAC), hIL-6 (F: CCACTCACCTCT TCAGAACG, R: CATCTTTGGAAGGTTCAGGTTG), hIL-10 (F: CAGAGTGAAGACTTTCTTTCAAATG, R: CCTTTAACAACAAGTTGTCCAGC); hRPLP0 (F: TAC ACCTTCCCACTTGCTGA, R: CCATATCCTCGTCCG ACTCC).

The relative gene expression quantification was performed using the comparative threshold (Ct) method (ΔΔCt), where relative gene expression level equals $2^{-\Delta\Delta Ct}$. The obtained fold changes in gene expression were normalized to the housekeeping gene RPLP0.

The real-time PCR data were processed by one-way ANOVA followed by Newman–Keuls post hoc test (GraphPad Prism Software version 5 Inc., San Diego, CA, USA). The data were expressed as the mean value ± standard deviation from three independent experiments. For all tested groups, the statistical significance was set up at $P < 0.05$.

### Statistical analysis

All the experiments were performed in triplicate. Data were expressed as mean ± SD. Differences between two experimental conditions were analyzed by unpaired Student's t test. Differences among three or more experimental samples were analyzed by ANOVA followed by Newman–Keuls post hoc test (GraphPad Prism Software version 5 Inc., San Diego, CA, USA). Significance was set at $P < 0.05$.

## Results

### Pericytes-like features of hDPSCs

Human dental pulp is a soft connective tissue entrapped within the pulp chamber of the tooth and is considered an interesting source of adult stem cells, i.e., hDPSCs. As shown in Fig. 2A, dental pulp tissue is largely vascularized as remarked by the immunohistochemical labeling
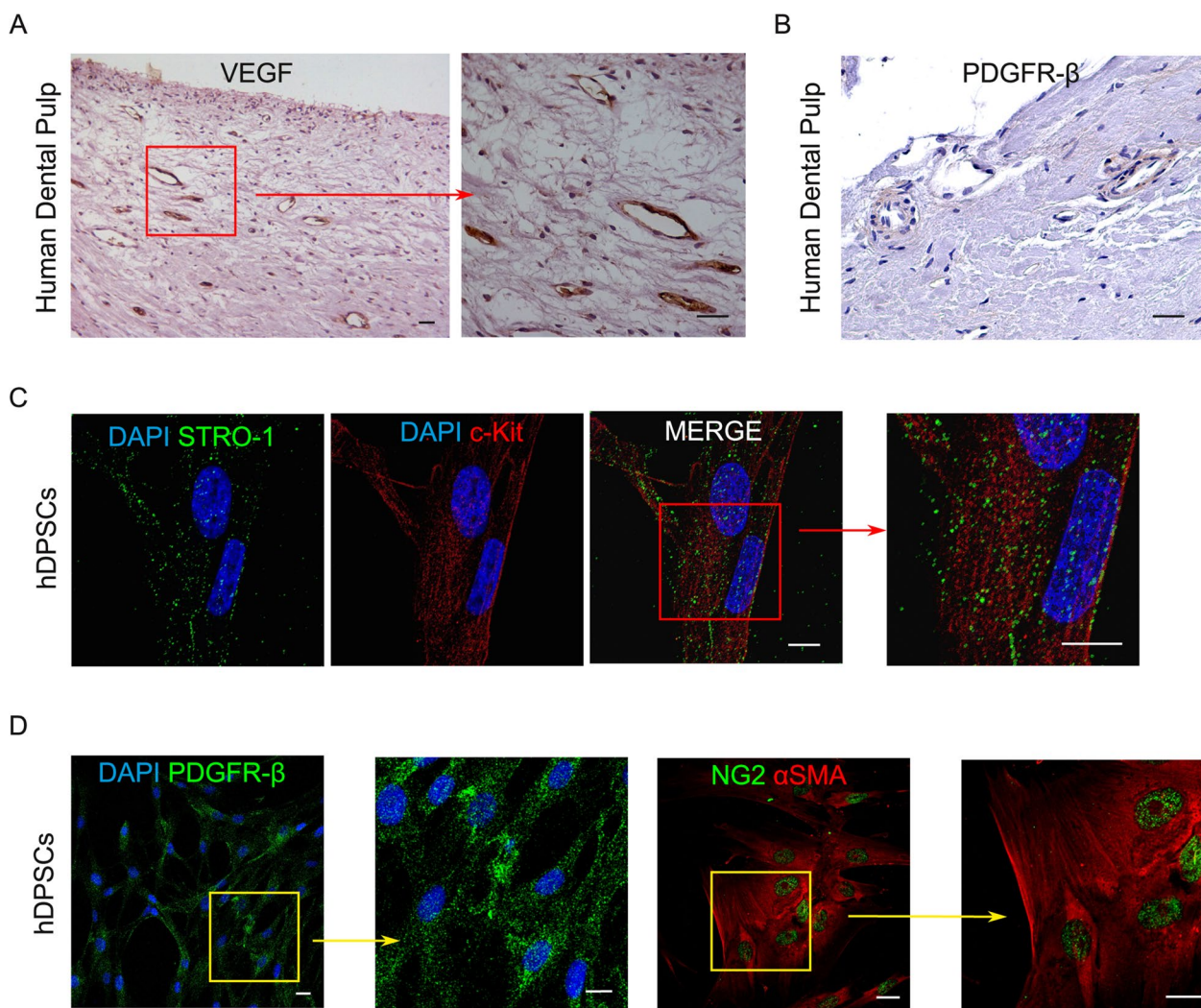
**Fig. 2** Immune-phenotypical characterization of hDPSCs. Immunohistochemistry of VEGF expression **A** and PDGFR-β **B** in human dental pulp tissue. Nuclei were counterstained with hematoxylin. Red square in A indicates higher magnification on the right. Scale bar: 50 μm. **C** Immunofluorescence analysis of STRO-1 and c-Kit in immune-selected hDPSCs. Red square indicates higher magnification highlighting the expression pattern of both markers. Scale bar: 10 μm. **D** Immunofluorescence analysis performed on STRO-1 + /c-Kit + hDPSCs shows the expression of PDGFR-β, NG2 and αSMA. Nuclei were stained with DAPI (blue). Yellow squares indicate higher magnifications of the related fields. Scale bar: 10 μm

against VEGF. Moreover, cells surrounding blood vessels express PDGFR-β, a typical pericyte marker (Fig. 2B). After dental pulp digestion, hDPSCs were isolated and expanded in vitro. Subsequently, through magnetic cell sorting, a pure stem cell population expressing STRO-1 and c-Kit was obtained and confirmed by immunofluorescence analysis (Fig. 2C). As reported in Fig. 1D, the immune-selected STRO-1+/c-Kit+hDPSCs population expressed PDGFR-β, NG2 and αSMA, confirming the pericyte-like cells phenotype (Fig. 2D).

**Angiogenic potential of pericytes-like cells**

Pericytes have been strongly associated with vessel formation and are involved in hemodynamic processes [26]. They are able to adhere to tissue culture plastic and to differentiate in vitro into different cell lineages [27]. The first aim of our study was to confirm the angiogenic abilities of hDPSCs. After 3, 5 and 7 days of induction toward endothelial differentiation, the commitment of hDPSCs was investigated through morphological, Western Blot and immunofluorescence analyses. Overall, during the
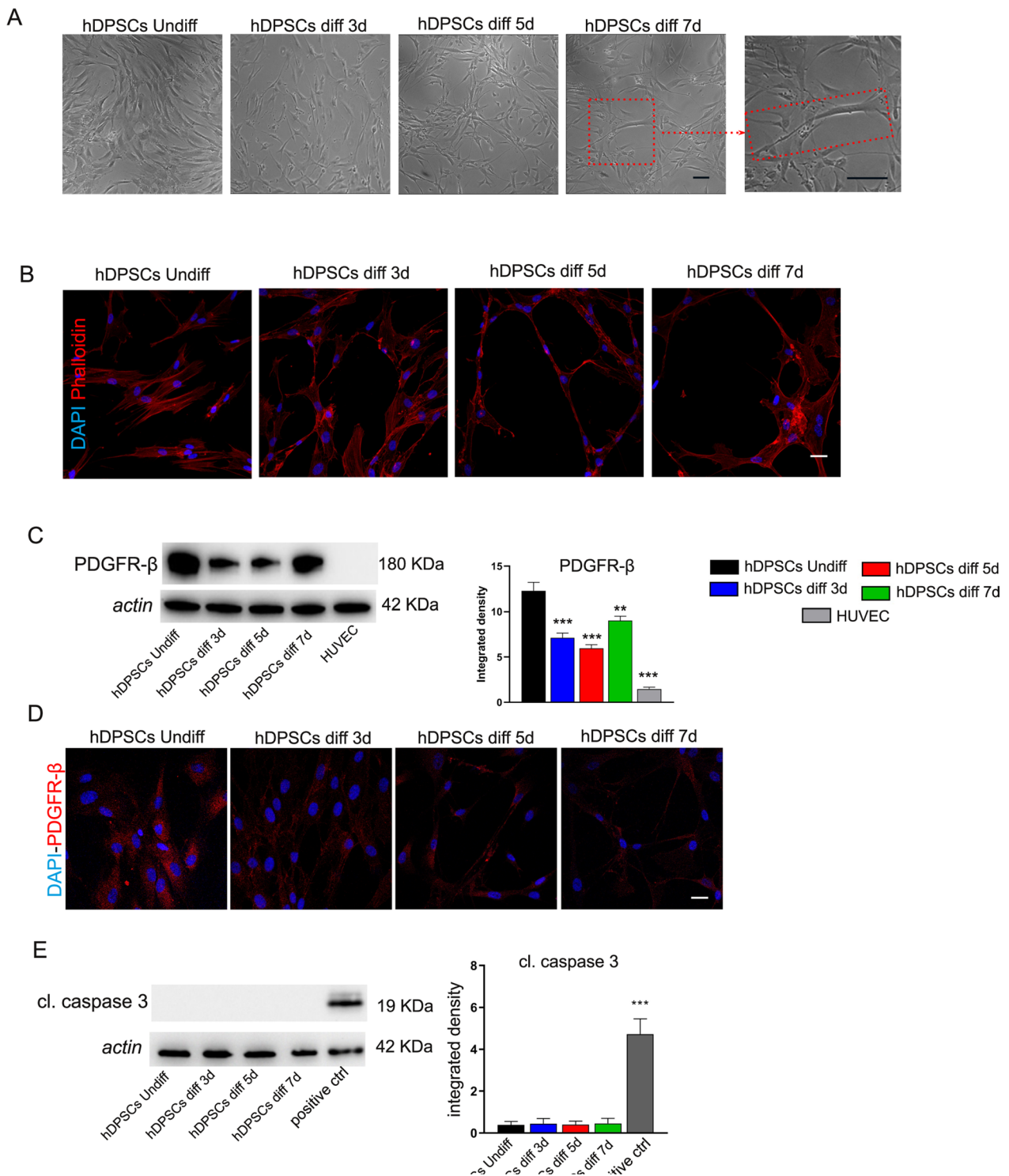
**Fig. 3** Endothelial differentiation of hDPSCs. **A** Morphological analysis of undifferentiated and endothelial differentiated hDPSCs after 3, 5 and 7 days of induction. Red dashed square and rectangle highlight the cord-like vessel morphology of differentiated hDPSCs. Scale bar: 50 μm. **B** Phalloidin staining shows the morphological rearrangement of hDPSCs toward endothelial lineage. Scale bar: 10 μm. **C–D** Western blot and immunofluorescence analyses of PDGFR-β in hDPSCs after endothelial differentiation. hDPSCs undiff and HUVEC were used as controls. **E** Western blot analysis of cleaved caspase 3 in hDPSCs following endothelial differentiation. Full-length blots are presented in Additional file 1: Figure S1A. Densitometry analysis is shown in histograms. Data are represented as mean ± SD, and statistical analysis on C and E was performed by one-way ANOVA followed by Dunnett post hoc test; ***$P < 0.001$, **$P < 0.01$ vs hDPSCs undiff ($n = 3$) (**C**), ***$P < 0.001$ positive ctrl vs hDPSCs ($n = 3$) (**E**)

Bertani *et al. Stem Cell Research & Therapy* (2023) 14:31

Page 8 of 16

induction of the endothelial differentiation, hDPSCs lost their typical fibroblast-like morphology. Morphological changes in elongated endothelial cells were appreciable after 3 and 5 days of commitment. After 7 days of induction, cells assembled into a linear cord-like vessel (Fig. 3A, red dashed rectangle, higher magnification). These data were further supported by phalloidin staining as shown in Fig. 3B. In parallel, WB analysis of differentiated hDPSCs revealed a statistically significant decrease in PDGFR-β expression when compared to undifferentiated hDPSCs (***$P < 0.001$; **$P < 0.01$ vs hDPSCs undiff). HUVEC cells do not express PDGFR-β confirming their endothelial phenotype (Fig. 3C; Additional File 1: Fig. S1A). This result is corroborated by immunofluorescence images reported in Fig. 3D.

Western blot analysis of cleaved caspase 3 showed that the endothelial induction did not affect cell viability of hDPSCs (***$P < 0.001$ vs hDPSCs; Fig. 3E; Additional File 1: Fig. S1A). The expression of typical endothelial markers ANGPT1, Tie2, eNOS and VEGF was also investigated. Interestingly, WB analysis revealed a statistically significant upregulation of eNOS and VEGF along the endothelial differentiation time, reaching similar expressions in HUVEC that were used as positive control (***$P < 0.001$, **$P < 0.01$, *$P < 0.05$ vs hDPSCs undiff). Regarding the expression of Tie2 receptor, a statistically significant increase was observed only at 7 days of induction (**$P < 0.01$ vs hDPSCs undiff), while no statistically significant differences were observed in its ligand, ANGPT1 (Fig. 4A; Additional File 1: Fig. S1B). These data were confirmed by immunofluorescence analysis reported in Fig. 4B. Remarkably, basal levels of all these endothelial markers were expressed in undifferentiated hDPSCs suggesting their tendency to angiogenic potential (Fig. 4A and B). As a matter of fact, a functional assay was performed in order to evaluate the ability of hDPSCs to form tube-like structures. As highlighted in Fig. 4C, the presence of tube-like vascular network formation was also observed in undifferentiated hDPSCs ($3 \pm 1.2$ tubes in $15 \times 10^3$ μm$^2$). This ability was strongly increased in hDPSCs upon the induction to endothelial differentiation ($20.5 \pm 1.73$ tubes in $15 \times 10^3$ μm$^2$, ***$P < 0.001$ vs hDPSCs undiff; Fig. 4C).

### Analysis of the effects mediated by flow-dependent shear stress

Blood vessels are regularly exposed to various types of hemodynamic forces (flow-dependent shear stress, FSS) induced by pulsatile blood flow and pressure. Shear stress can play a critical role in vascular homeostasis and remodeling as well as in the pathophysiology process by acting on endothelial cells and/or pericytes [28]. Many cellular structures, including cell membrane that

represents the first layer exposed to external stimuli, respond to shear stress by adapting their shape. Based on this consideration, we noticed that hDPSCs exposed to FSS rearranged their morphology (Fig. 5A). Cells consequently appeared more elongated, losing their typical fibroblast-like morphology (Fig. 5A, black arrows). In order to exclude the possibility that FSS induced an alteration in stemness phenotype, FACS analysis was carried out on hDPSCs cultured in standard static conditions and on hDPSCs exposed to FSS, i.e., dynamic conditions. Our results showed that the FSS did not alter the expression of typical MSCs markers on hDPSCs from both experimental groups. Indeed, as reported in Fig. 5B almost all hDPSCs were positive for CD73, CD90 and CD105 while being negative for CD34, CD45 and HLA-DR (Fig. 5B).

Following the initial mechanosensing reflected on hDPSCs membrane modifications, the activation of local biochemical responses and downstream intracellular signaling pathways might have occurred [29]. In particular, we evaluated different activated pathways on hDPSCs exposed to FSS. As shown in Fig. 6A, heatmap and histograms revealed the activation of different signaling mechanisms. First of all the FSS did not induce pro-apoptotic signaling in hDPSCs as revealed by the lack of variation in the expression of cleaved PARP protein in both experimental groups. The major finding of the present analysis is that Akt/mTOR pathway was activated in response to pulsatile unidirectional flow-dependent shear stress. As shown, the statistical up-regulation of Akt pS473 was correlated with the statistically significant increase in mTOR pS2481 in hDPSCs under dynamic conditions when compared to hDPSCs under static conditions (***$P < 0.001$, **$P < 0.01$ dynamic condition vs static condition). In parallel, the phosphorylation of Akt pT308 did not change in both experimental conditions and the phosphorylation of PDK1 s241 decreased in statistically significant manner in hDPSCs exposed to FSS (***$P < 0.001$ vs static condition). These data indicate the Akt/mTOR pathway activation is due to hDPSCs membrane deformation and mechanosensing activation. Moreover, remarkably the FSS induced a statistically significant decrease in PD-L1 immunomodulatory marker. In parallel, hDPSCs maintained in dynamic conditions displayed a strong up-regulation of NFkB pS536, along with a statistically significant decrease in IKBα pS32 36, whose phosphorylation is reported to be linked with NFkB inactivation (***$P < 0.001$ vs static condition). These data could suggest that pulsatile flow shear stress regulates the pro-inflammatory fate of hDPSCs. Interestingly, we noticed that the FSS induced a statistically significant downregulation of eNOS pS117 (***$P < 0,001$ vs static condition) and in parallel a statistical significant up-regulation of
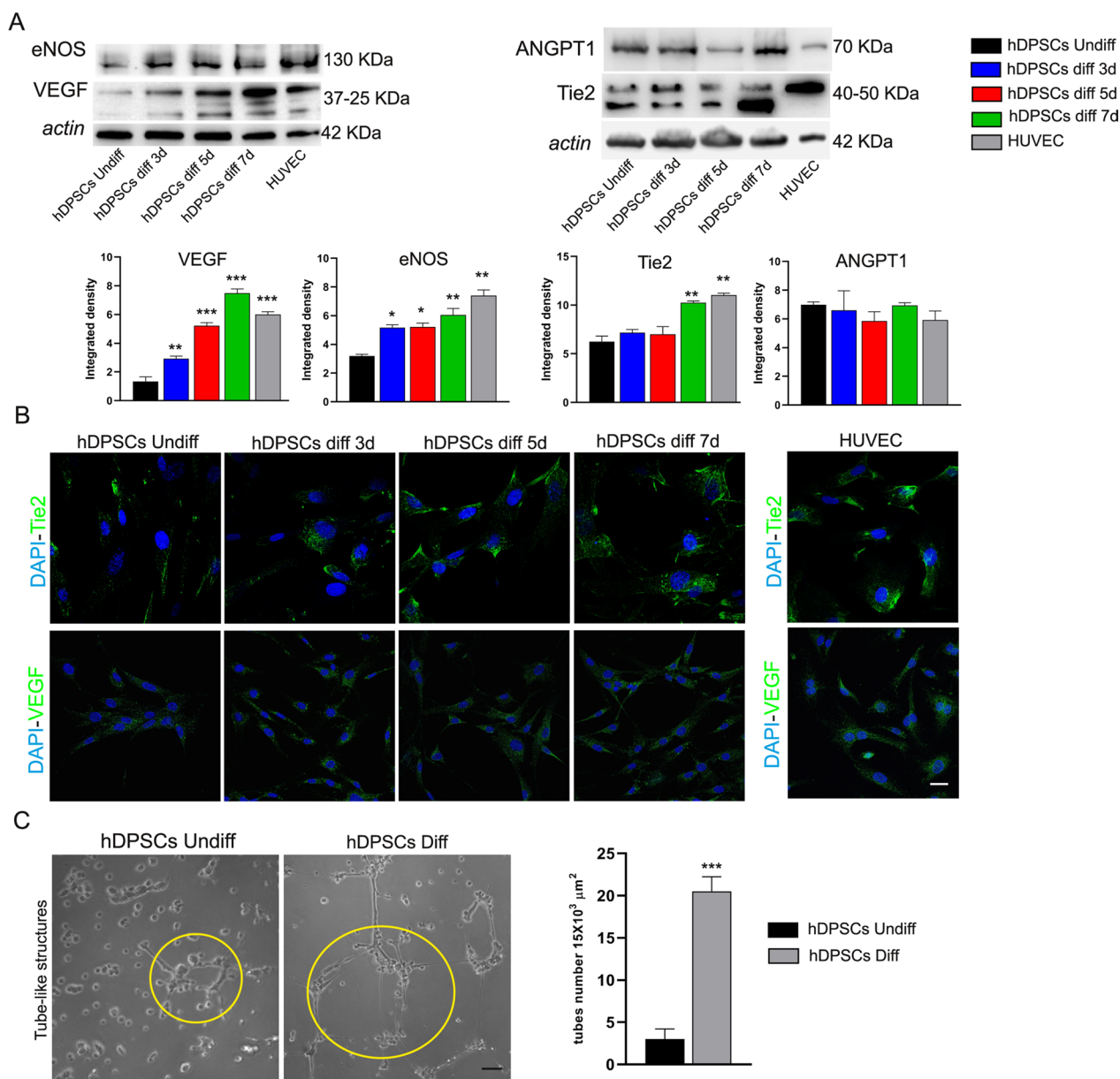
Bertani *et al. Stem Cell Research & Therapy*    (2023) 14:31

Page 9 of 16



**Fig. 4** Evaluation of angiogenic potential of hDPSCs. **A** Western blot analysis of eNOS, VEGF, ANGPT1 and Tie2 in endothelial differentiated hDPSCs. hDPSCs undiff and HUVEC were used as controls. Full-length blots are reported in Additional file 1: Figure S1B. **B** The expression of Tie2 and VEGF is shown by immunofluorescence images. Nuclei were counterstained with DAPI. Scale bar: 10 μm. **C** Tube formation assay showing tube-like structures in undifferentiated and endothelial differentiated hDPSCs. Histograms reporting the mean ± SD number of tube-like structures in $15 \times 10^3$ μm$^2$. Scale bar: 50 μm. Data are represented as mean ± SD, and statistical analysis on A was performed by one-way ANOVA followed by Dunnett post hoc test; ***$P < 0.001$, **$P < 0.01$, *$P < 0.05$ vs hDPSCs undiff ($n = 3$). Statistical analysis on C was carried out by unpaired Student's t test; ***$P < 0.001$ vs hDPSCs undiff ($n = 3$)

eNOS pS113 (***$P < 0,001$ vs static condition). These data suggest that eNOS activity was inhibited as well as FSS affect angiogenic potential tendency of hDPSCs. This data was confirmed by immunofluorescence staining of typical angiogenic markers (VEGF, ANGPT1 and eNOS) and by tube formation assay. In particular

as revealed by pseudocolor analysis, the expression of VEGF, ANGPT1 and eNOS decreased in hDPSCs exposed to dynamic culture conditions (Fig. 6B). At the same time, the functional analysis also revealed a statistically significant reduction in the count of tube-like structures in hDPSCs under dynamic condition
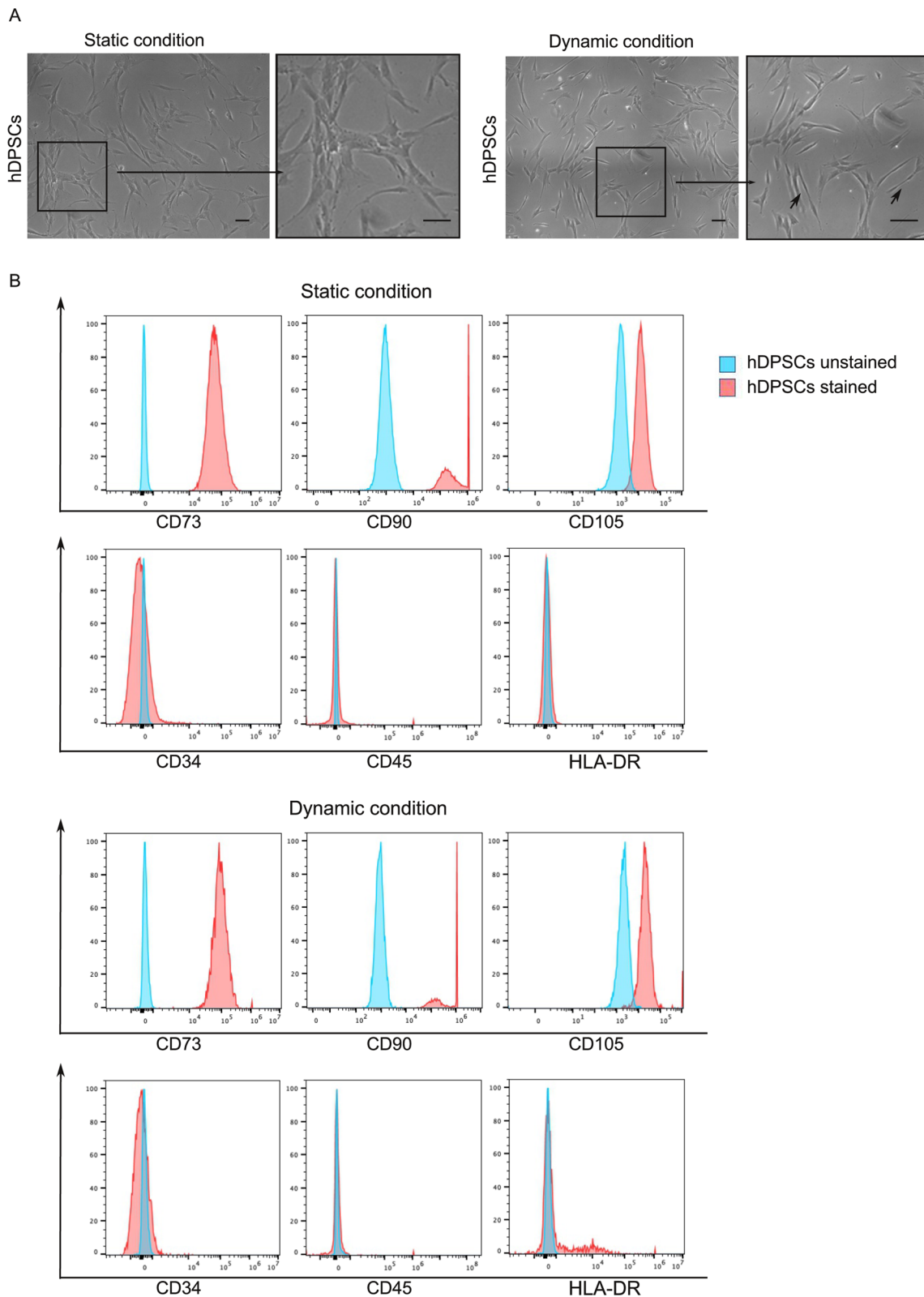
**Fig. 5** Unidirectional pulsatile flow shear stress effects on hDPSCs. **A** Evaluation of hDPSCs morphology after culture under static and dynamic conditions. Black squares and arrows indicate higher magnification and cell morphology, respectively. Scale bar: 50 µm. **B** FACS analysis of MSCs typical markers (CD73, CD90, CD105, CD34, CD45, HLA-DR) on hDPSCs after static and dynamic culture conditions

Bertani *et al. Stem Cell Research & Therapy*     (2023) 14:31

Page 11 of 16

(0.5 ± 0.5 tubes in $15 \times 10^3$ μm$^2$; ***$P < 0.001$) when compared with the hDPSCs maintained in static culture condition (21 ± 1.5 tubes in $15 \times 10^3$ μm$^2$; Fig. 6C), thus confirming that the FSS also influenced the ability of hDPSCs to form tube-like vascular networks and subsequently their angiogenic potential.

### Analysis of the immunomodulatory and inflammatory response of hDPSCs to flow-dependent shear stress

The effect of dynamic flow conditions on the inflammatory microenvironment mimicked by the co-culture between hDPSCs and pre-activated CD3/CD28 hPBMCs was investigated (Fig. 7A). The biological analysis was carried out by RPPA on hDPSCs after co-culture with PBMCs with or without FSS. As demonstrated above, we first confirmed that mechanosensing transduction activated the pathway of Akt/mTOR. Particularly, as reported in Fig. 7A, histograms showed a statistically significant increase in Akt pS473 that correlated with a statistically significant increase in mTOR pS2481 in hDPSCs under dynamic conditions, when compared to hDPSCs under static conditions (***$P < 0.001$ hDPSCs dynamic condition vs hDPSCs static condition). Moreover, no statistically significant difference was detected in the phosphorylation of Akt pT308 in both experimental conditions, whereas the phosphorylation of PDK1 S241 statistically significant decreased in hDPSCs after co-culture with PBMCs exposed to FSS (***$P < 0.001$ vs static condition). In this co-culture system, the eNOS activity of hDPSCs exposed to FSS was inhibited, as demonstrated by the significant downregulation of eNOS pS117 (***$P < 0.001$ vs hDPSCs static condition) and, at the same time, by the statistically significant upregulation of eNOS pS113 (***$P < 0.001$ vs hDPSCs static condition, Fig. 7A). Subsequently, we investigated the immunomodulatory properties in hDPSCs exposed or not to FSS after co-culture with PBMCs. Interestingly, the upregulation of PD-L1 was confirmed in hDPSCs in static condition in accordance with our previous findings. The application of FSS drastically decreased (more than 60%) the expression of PD-L1 in hDPSCs in dynamic condition when compared to hDPSCs in static condition (***$P < 0.001$ vs static condition; Fig. 7A). At the same time, an evident increase in NFkB pS536, as well as a significant reduction of IKBα

pS32 36, was revealed in hDPSCs under dynamic condition after co-culture with PBMCs (***$P < 0.001$ vs static condition; Fig. 7A), suggesting that a pro-inflammatory fate is driven by FSS.

In order to confirm the plasticity of hDPSCs in immunomodulation, we evaluated the intracellular inflammatory cytokines in pre-activated PBMCs after co-culture with hDPSCs in static and dynamic condition. To this regard, FACS analysis showed a minimal and comparable contamination of hDPSCs in PBMCs after either static or dynamic co-culture (Fig. 7B). In detail, the FSS was able to induce an up-regulation trend of mRNA expression levels of all cytokines tested in pre-activated PBMCs alone in dynamic conditions when compared to the counterpart in static conditions. Furthermore, histograms showed a strong significant increase in mRNA expression levels of IFNγ, TNFα, IL-2, IL-10 and IL-6 in PBMCs after hDPSCs co-culture in dynamic condition (°°°$P < 0.001$, °$P < 0.05$ vs PBMCs after hDPSCs co-culture in static condition, Fig. 7C). Conversely, a downregulation of cytokines levels (IFNγ, TNFα, IL-2, IL-10) was detected in PBMCs after hDPSCs co-culture in static condition, when compared with PBMCs cultured alone in static condition (*$P < 0.05$; Fig. 7C), except for IL-6 that was up-regulated (***$P < 0.001$) after hDPSCs co-culture in static condition, which is in accordance with our previous findings (Fig. 7C) [7, 12]. Taken together these data suggest that FSS exerted a strong effect on pro-inflammatory behavior of hDPSCs.

## Discussion

Pericytes are mural cells that surround the endothelium of small vessels. They regulate numerous functions including vessel growth, stabilization and permeability [30]. Defining a pericyte is a challenge since no unique molecular marker has been identified because of the different embryological origin, functions and locations in various tissues. A large number of studies have suggested that pericytes behave as MSCs. Indeed, besides the expression of PDGFRβ, pericytes express typical MSCs markers, are able to adhere to tissue culture plastic, can be expanded in vitro for multiple passages and can differentiate into different cell lineages. [27, 31]. Pericytes have

(See figure on next page.)

**Fig. 6** Mechanotransduction induced in hDPSCs by FSS. **A** Heatmap of RPPA analysis carried out on phosphorylated proteins in hDPSCs, after static and dynamic conditions. Histograms showing the most prominent signaling pathways. Data are represented as mean ± SD, and statistical analysis was carried out by unpaired Student's t test; ***$P < 0.001$, **$P < 0.01$ vs hDPSCs in static condition ($n = 5$). **B** Immunofluorescence analysis carried out on hDPSCs, under static and dynamic conditions, shows the expression of endothelial markers VEGF, ANGPT1 and eNOS. Pseudocolor analysis of each endothelial marker is reported on the right side. Nuclei were counterstained by DAPI. Scale bar: 10 μm. **C** Tube formation assay showing tube-like structures in endothelial differentiated hDPSCs under static and dynamic conditions. Histograms reporting the mean ± SD number of tube-like structures in $15 \times 10^3$ μm$^2$. Scale bar: 50 μm. Data are represented as mean ± SD and statistical analysis was carried out by unpaired Student's t test; ***$P < 0.001$ vs hDPSCs diff static condition ($n = 5$)
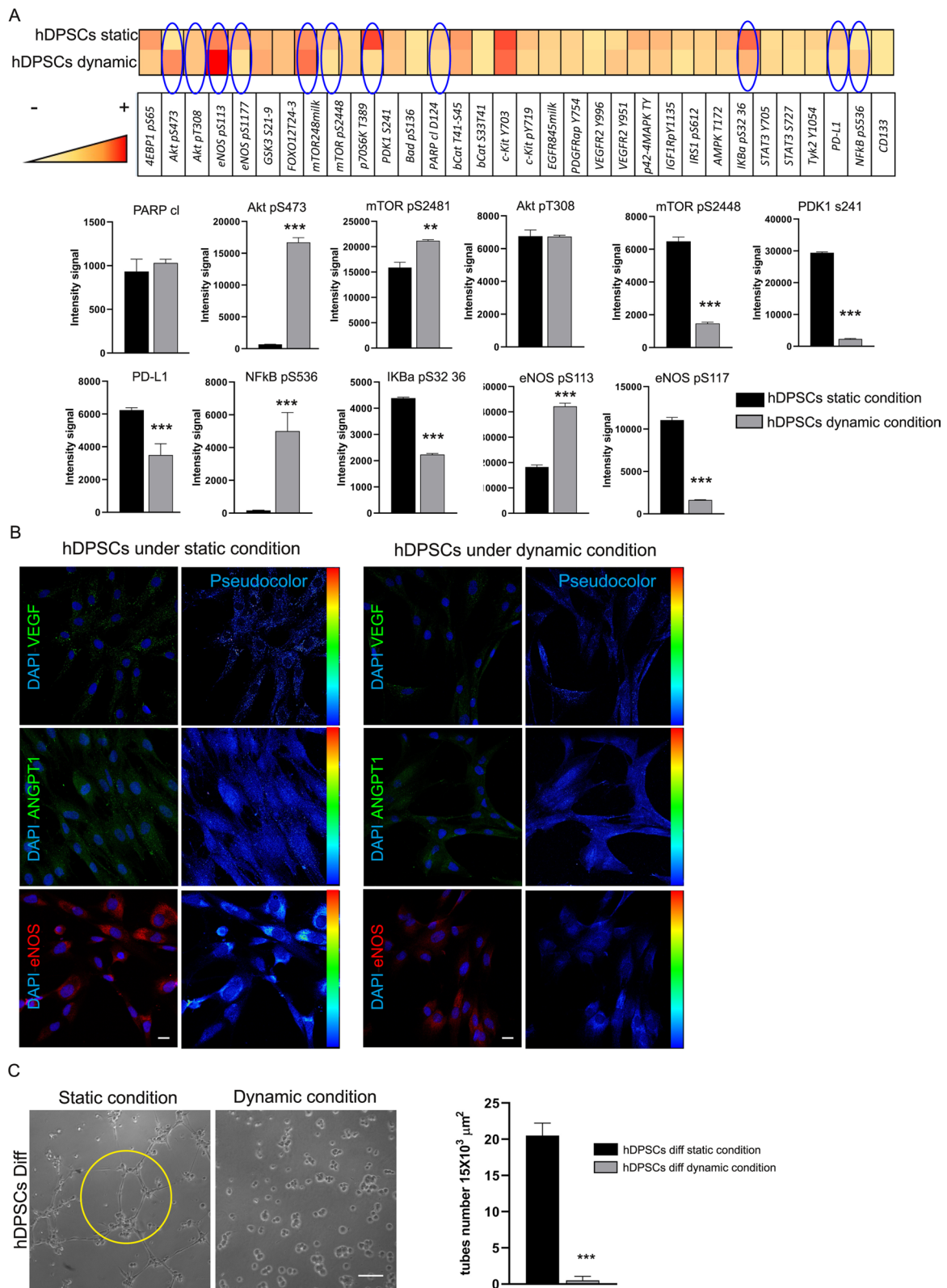
**Fig. 6** (See legend on previous page.)

been strongly associated with vessel formation and stabilization as well as hemodynamic processes of blood vessels, and it is suggested that either direct and paracrine interplay between pericytes and endothelial cells exists [3, 32–36]. It is well known that pericytes have an angiogenic and vasculogenic potential in enhancing blood vessel formation [37].

In our study, we have demonstrated that STRO-1+/c-Kit+human dental pulp stem cells are able to express both typical MSCs markers and PDGFRβ, suggesting their pericyte-like phenotype, in accordance with previous findings [13, 38].

In the first phase of our study, we have observed that hDPSCs are able to express at basal levels, in undifferentiated status, the typical endothelial markers, i.e., Tie2, eNOS, ANGPT1 and VEGF that are upregulated after culture in the endothelial induction medium, thus confirming that hDPSCs are naturally prone toward endothelial differentiation. These findings are supported by the ability of hDPSCs to form tube-like structures as early as in undifferentiated status. Notably, angiogenic signaling including ANGPT1 and Tie2 was detected in hDPSCs in standard conditions and maintained also after endothelial induction. To this regard, it is well known that ANGPT1/Tie2 signaling is able to regulate two opposite processes, i.e., vascular quiescence and angiogenesis [39], and has also been proven to exert potent anti-inflammatory effects, by inhibiting NF-kB, a transcription factor involved in inflammatory processes [40].

Interestingly, the ANGPT1/Tie2 signaling might be influenced by mechanical forces including pulsatile shear stress, suggesting that FSS plays a pivotal role in modulating the endothelial phenotype of pericyte-like cells and, likely, their immunomodulatory/inflammatory behavior as well [28]. Our data demonstrate that when a pulsatile unidirectional flow is applied to hDPSCs their stemness phenotype was not altered, however a shift in cell morphology was observed. As a matter of fact, it is well known that fluid shear stress induces deformation of cell membranes. This event, called mechanosensing, consists in the transformation of mechanical stress into biochemical signals, inducing the activation of downstream intracellular signaling pathways, alterations of gene and protein expression, which result in modification of cell function [29].

In light of our results, the endothelial differentiation potential of hDPSCs exposed to FSS was inhibited as shown by the downregulation of pro-angiogenic phosphorylation of eNOS S1177 [31] and the simultaneous upregulation of anti-angiogenic phosphorylation of eNOS S113 [42]. Moreover, we observed a decreased expression of VEGF and ANGPT1 as well as the loss of tube formation ability. Our findings highlighted that these cell functional alterations are strictly related to mechanically dependent activation of biochemical signaling pathways, as demonstrated either by the increased expression of Akt pS473/mTOR pS2481 and the lack of activation in Akt pT308/mTOR pS2448, in accordance with findings from Dimmeler et al. [43]

It is noteworthy that the pulsatile unidirectional flow application induced the downregulation of the immune-modulatory molecule PD-L1. As demonstrated by our recent studies, hDPSCs are able to modulate the inflammatory microenvironment by exerting immunomodulatory properties through the upregulation of PD-L1 [8].

This downregulation might reflect hDPSCs plasticity in exerting immunomodulation, switching their potential from an anti-inflammatory toward a pro-inflammatory fate. The latter one might indeed be linked to the observed upregulation of NFkB pS536 [44].

To this purpose, we aimed to further demonstrate our hypothesis by co-culturing hDPSCs in an inflammatory microenvironment in the presence of FSS. Evidence from these culture conditions confirmed the data observed above and the upregulation of PD-L1 was observed in hDPSCs maintained in static co-culture conditions, thus confirming our previous findings [7]. Interestingly, when FSS was applied to hDPSCs/PBMCs co-culture, a significant reduction of PD-L1 was detected, together with a stronger upregulation of NFkB pS536. These data strengthen the ability of flow-dependent shear stress to modulate the immunomodulatory features of hDPSCs that, when also exposed to an inflammatory microenvironment mimicked by pre-activated PBMCs, further drop their potential to express immunomodulatory molecules and, at the same time, move toward a pro-inflammatory behavior.

Additional proof of this event resulted from the significantly up-regulated expression levels of all the

(See figure on next page.)

**Fig. 7** Effects of inflammatory microenvironment on hDPSCs exposed to FSS. **A** Heatmap of RPPA analysis carried out on phosphorylated proteins in hDPSCs, after co-culture with PBMCs in static and dynamic conditions. Histograms showing the most prominent signaling pathways. Data are represented as mean ± SD, and statistical analysis was carried out by unpaired Student's *t* test; \*\*\**P* < 0.001, \*\**P* < 0.01 vs hDPSCs in static condition (*n* = 5). **B** FACS analysis of CD45 on PBMCs following static and dynamic co-culture with hDPSCs. **C** Real-time PCR analysis of different cytokines was performed on PBMCs after hDPSCs co-culture in static and dynamic conditions. Histograms represent the mean ± SD mRNA fold-change (*n* = 5). Statistical analysis was carried out by one-way ANOVA followed by Newman–Keuls post hoc test. \*\*\**P* < 0.001, \*P < 0.05 vs. PBMCs alone in static condition; °°°*P* < 0.001, °P < 0.05 vs PBMCs after DPSCs co-culture in static conditions
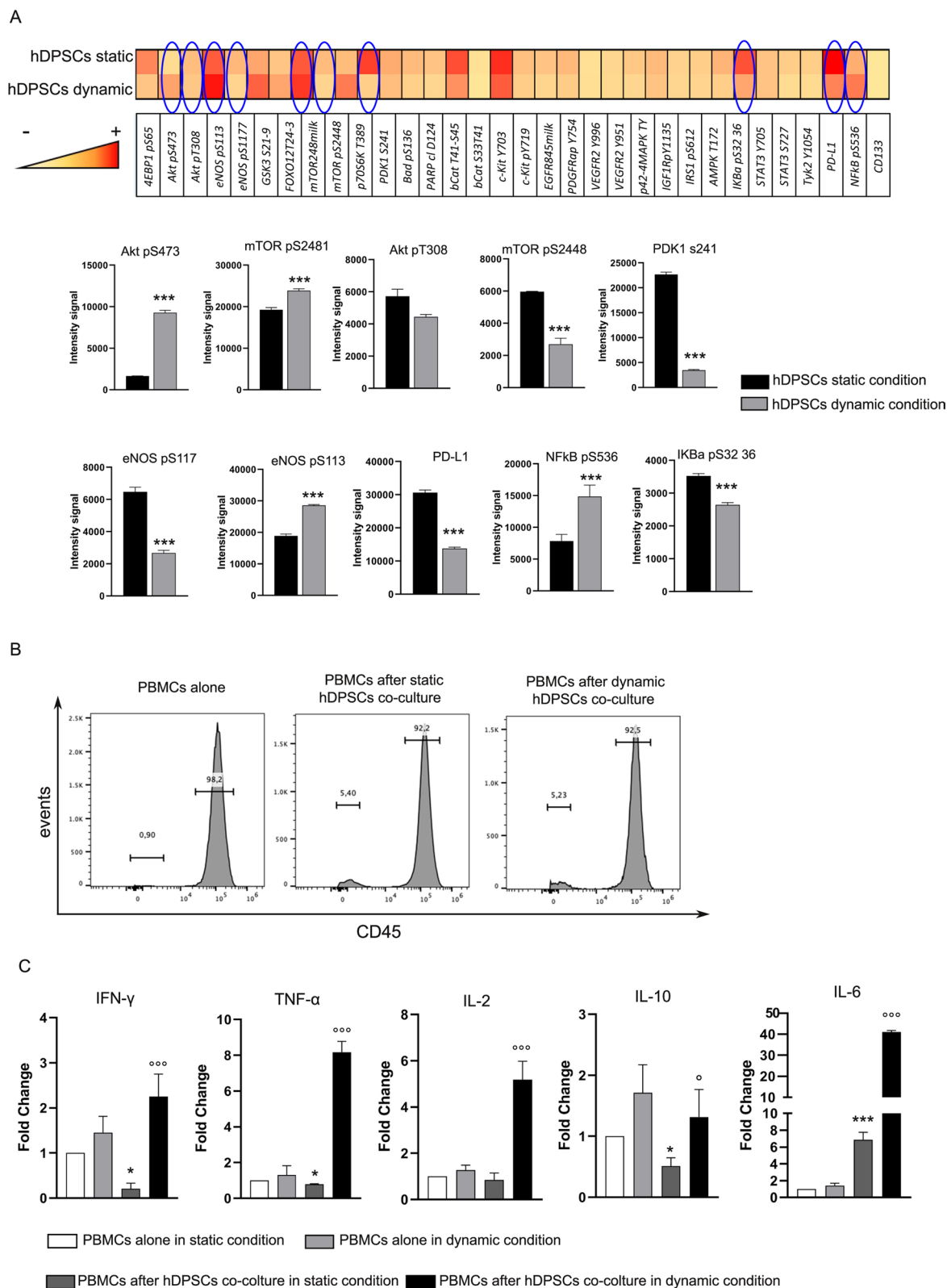
**Fig. 7** (See legend on previous page.)

Bertani *et al. Stem Cell Research & Therapy*       (2023) 14:31

Page 15 of 16

evaluated pro-inflammatory cytokines expressed by PBMCs. These findings are definitely countertrend when compared to data obtained from co-culture experiments in static conditions, which are still consistent with evidence from our recent studies [7, 12].

## Conclusions
Taken together all these observations, it might be argued that mechanical forces may determine the biological fate of hDPSCs, which might be activated during the development of diseases driven by the establishment of an inflammatory microenvironment, such as autoimmune diseases and precancerous lesions. To this regard, it is known that MSCs hold an active interplay with immune cells and consequently may display both anti-inflammatory and pro-inflammatory effects by acting as sensors and switchers of inflammation [45]. Moreover, these data pave the way to understand the potential role of pericyte-like cells and mechanical forces in the trigger and development of inflammation-dependent diseases.

## Supplementary Information
The online version contains supplementary material available at https://doi.org/10.1186/s13287-023-03254-2.

---
**Additional file 1: Figure S1.** Extended data for figure 3 and 4. Uncropped Western blot images showing **A** PDGFR-β and related actin; **B** cleaved caspase-3 and related actin; **C** eNOS and VEGF with related actin; **D** Tie2, ANGPT1 and related actin. Boxed areas correspond to cropped regions shown in figure 3C and 3E. Specific target bands were selected according to the molecular weight reported in antibodies' datasheets. **Table S1**: raw RPPA data.

---

### Author contributions
GB, RDT and LB contributed to investigation, methodology and writing—original draft preparation; AP, RR and LR were involved in data curation, validation and writing—original draft preparation; GO contributed to investigation and writing—original draft; MS and SDB were involved in investigation and writing—review and editing; JB and PS contributed to resources and writing—review and editing; and EV and GC were involved in conceptualization, writing—original draft preparation, funding acquisition and supervision. All authors read and approved the final manuscript.

### Availability of data and materials
All data generated or analyzed during this study are included in this article.

## Declarations

### Ethics approval and consent to participate
The study was performed according to the recommendations of Comitato Etico Provinciale-Azienda Ospedaliero-Universitaria di Modena (Modena, Italy) ref. number 3299/CE; 5 September 2017.

### Consent for publication
Not applicable.

### Competing interests
The authors declare that no competing interests exist.

### Author details
¹Department of Surgery, Medicine Dentistry and Morphological Sciences With Interest in Transplant, University of Modena and Reggio Emilia, Modena, Italy. ²Department of Engineering Sciences and Methods, University of Modena and Reggio Emilia, Modena, Italy. ³Department of Chemical and Geological Sciences, University of Modena and Reggio Emilia, Modena, Italy. ⁴RPPA Unit, Proteomics Area, Core Facilities, Istituto Superiore di Sanità, Rome, Italy. ⁵Department of Medical and Surgical Sciences for Children and Adults, University of Modena and Reggio Emilia, Modena, Italy.

## References
1. Rucker HK, Wynder HJ, Thomas WE. Cellular mechanisms of CNS pericytes. Brain Res Bull. 2000;51:363–9.
2. Ribatti D, Nico B, Crivellato E. The role of pericytes in angiogenesis. Int J Dev Biol. 2011;55:261–8.
3. Ozerdem U, Stallcup WB. Early contribution of pericytes to angiogenic sprouting and tube formation. Angiogenesis. 2003;6:241–9.
4. Carmeliet P. Manipulating angiogenesis in medicine. J Intern Med. 2004;255:538–61.
5. Harrell CR, Simovic Markovic B, Fellabaum C, Arsenijevic A, Djonov V, Volarevic V. Molecular mechanisms underlying therapeutic potential of pericytes. J Biomed Sci. 2018;25:21.
6. Goettsch W, Gryczka C, Korff T, Ernst E, Goettsch C, Seebach J, et al. Flow-dependent regulation of angiopoietin-2. J Cell Physiol. 2008;214(2):491–503.
7. Yianni V, Sharpe PT. Transcriptomic profiling of dental pulp pericytes: an RNAseq approach. Front Dental Med. 2020;1:6.
8. Di Tinco R, Bertani G, Pisciotta A, Bertoni L, Pignatti E, Maccaferri M, et al. Role of PD-L1 in licensing immunoregulatory function of dental pulp mesenchymal stem cells. Stem Cell Res Ther. 2021;12:598.
9. Zordani A, Pisciotta A, Bertoni L, Bertani G, Vallarola A, Giuliani D, et al. Regenerative potential of human dental pulp stem cells in the treatment of stress urinary incontinence: in vitro and in vivo study. Cell Prolif. 2019;52: e12675.
10. Pisciotta A, Bertoni L, Riccio M, Mapelli J, Bigiani A, Noce ML, et al. Use of a 3D floating sphere culture system to maintain the neural crest-related properties of human dental pulp stem cells. Front Physiol. 2018;9:547.
11. Carnevale G, Pisciotta A, Riccio M, Bertoni L, De Biasi S, Gibellini L, et al. Human dental pulp stem cells expressing STRO-1, c-kit and CD34 markers in peripheral nerve regeneration. J Tissue Eng Regen Med. 2016;12:e774–85.
12. Pisciotta A, Riccio M, Carnevale G, Lu A, De Biasi S, Gibellini L, et al. Stem cells isolated from human dental pulp and amniotic fluid improve skeletal muscle histopathology in mdx/SCID mice. Stem Cell Res Ther. 2015;6:1–5.
13. Croci S, Bonacini M, Dolci G, Massari M, Facciolongo N, Pignatti E, Production HDPSCMC, in vitro by Peripheral Blood Mononuclear Cells From Coronavirus Disease, et al. Patients. Front Cell Develop Biol. 2019;2021:8.
14. Pisciotta A, Bertani G, Bertoni L, Di Tinco R, De Biasi S, Vallarola A, et al. Modulation of cell death and promotion of chondrogenic differentiation by fas/fasl in human dental pulp stem cells (hDPSCs). Front Cell Develop Biol. 2020;8:279.
15. Kizil C, Kyritsis N, Brand M. Effects of inflammation on stem cells: together they strive? EMBO Rep. 2015;16:416–26.
16. Pizzicannella J, Pierdomenico SD, Piattelli A, Varvara G, Fonticoli L, Trubiani O, et al. 3D human periodontal stem cells and endothelial cells promote bone development in bovine pericardium-based tissue biomaterial. Materials (Basel). 2019;12:E2157.

Bertani *et al. Stem Cell Research & Therapy*    (2023) 14:31

Page 16 of 16

17. Xie X, Wang F, Zhu L, Yang H, Pan D, Liu Y, et al. Low shear stress induces endothelial cell apoptosis and monocyte adhesion by upregulating PECAM-1 expression. Mol Med Rep. 2020;21(6):2580–3258.

18. 'T Hart DC, van der Vlag J , Nijenhuis T Laminar flow substantially affects the morphology and functional phenotype of glomerular endothelial cells. PLoS One 2021;16(5): e0251129.

19. Conserva E, Pisciotta A, Borghi F, Nasi M, Pecorini S, Bertoni L, et al. Titanium surface properties influence the biological activity and fasl expression of craniofacial stromal cells. Stem Cells Int. 2019;2019:4670560.

20. VanMeter A, Signore M, Pierobon M, Espina V, Liotta LA, Petricoin EF. Reverse-phase protein microarrays: application to biomarker discovery and translational medicine. Expert Rev Mol Diagn. 2007;7:625–33.

21. Signore M, Alfonsi R, Federici G, Nanni S, Addario A, Bertuccini L, et al. Diagnostic and prognostic potential of the proteomic profiling of serum-derived extracellular vesicles in prostate cancer. Cell Death Dis. 2021;12:636.

22. Kielkopf CL, Bauer W, Urbatsch IL. bradford assay for determining protein concentration. Cold Spring Harb Protoc. 2020;2020: 102269.

23. Laemmli UK. Cleavage of structural proteins during the assembly of the head of bacteriophage T4. Nature. 1970;227:680–5.

24. Bobrow MN, Harris TD, Shaughnessy KJ, Litt GJ. Catalyzed reporter deposition, a novel method of signal amplification. Appl Immunoassays J Immunol Methods. 1989;125:279–85.

25. Signore M, Manganelli V, Hodge A. Antibody Validation by Western Blotting. Methods Mol Biol. 2017;1606:51–70.

26. Bergers G, Song S. The role of pericytes in blood-vessel formation and maintenance. Neuro Oncol. 2005;7:452–64.

27. Crisan M, Yap S, Casteilla L, Chen C-W, Corselli M, Park TS, et al. A perivascular origin for mesenchymal stem cells in multiple human organs. Cell Stem Cell. 2008;3:301–13.

28. Yang Z, Xia W-H, Zhang Y-Y, Xu S-Y, Liu X, Zhang X-Y, et al. Shear stress-induced activation of Tie2-dependent signaling pathway enhances reendothelialization capacity of early endothelial progenitor cells. J Mol Cell Cardiol. 2012;52:1155–63.

29. Chiu J-J, Usami S, Chien S. Vascular endothelial responses to altered shear stress: pathologic implications for atherosclerosis. Ann Med. 2009;41:19–28.

30. Cappellari O, Cossu G. Pericytes in development and pathology of skeletal muscle. Circ Res. 2013;113:341–7.

31. Dellavalle A, Sampaolesi M, Tonlorenzi R, Tagliafico E, Sacchetti B, Perani L, et al. Pericytes of human skeletal muscle are myogenic precursors distinct from satellite cells. Nat Cell Biol. 2007;9:255–67.

32. Ozerdem U, Grako KA, Dahlin-Huppe K, Monosov E, Stallcup WB. NG2 proteoglycan is expressed exclusively by mural cells during vascular morphogenesis. Dev Dyn. 2001;222:218–27.

33. Reynolds LP, Grazul-Bilska AT, Redmer DA. Angiogenesis in the corpus luteum. Endocrine. 2000;12:1–9.

34. Enge M, Bjarnegård M, Gerhardt H, Gustafsson E, Kalén M, Asker N, et al. Endothelium-specific platelet-derived growth factor-B ablation mimics diabetic retinopathy. EMBO J. 2002;21:4307–16.

35. Hellström M, Kalén M, Lindahl P, Abramsson A, Betsholtz C. Role of PDGF-B and PDGFR-beta in recruitment of vascular smooth muscle cells and pericytes during embryonic blood vessel formation in the mouse. Development. 1999;126:3047–55.

36. Hirschi KK, Rohovsky SA, Beck LH, Smith SR, D'Amore PA. Endothelial cells modulate the proliferation of mural cell precursors via platelet-derived growth factor-BB and heterotypic cell contact. Circ Res. 1999;84:298–305.

37. Xu J, Gong T, Heng BC, Zhang CF. A systematic review: differentiation of stem cells into functional pericytes. FASEB J. 2017;31:1775–86.

38. Feng J, Mantesso A, De Bari C, Nishiyama A, Sharpe PT. Dual origin of mesenchymal stem cells contributing to organ growth and repair. Proc Natl Acad Sci USA. 2011;108:6503–8.

39. Fukuhara S, Sako K, Noda K, Zhang J, Minami M, Mochizuki N. Angiopoietin-1/Tie2 receptor signaling in vascular quiescence and angiogenesis. Histol Histopathol. 2010;25:387–96.

40. Hughes DP, Marron MB, Brindle NPJ. The antiinflammatory endothelial tyrosine kinase Tie2 interacts with a novel nuclear factor-kappaB inhibitor ABIN-2. Circ Res. 2003;92:630–6.

41. Chen C-A, Druhan LJ, Varadharaj S, Chen Y-R, Zweier JL. Phosphorylation of endothelial nitric-oxide synthase regulates superoxide generation from the enzyme. J Biol Chem. 2008;283:27038–47.

42. Lee C-H, Wei Y-W, Huang Y-T, Lin Y-T, Lee Y-C, Lee K-H, et al. CDK5 phosphorylates eNOS at Ser-113 and regulates NO production. J Cell Biochem. 2010;110:112–7.

43. Dimmeler S, Assmus B, Hermann C, Haendeler J, Zeiher AM. Fluid shear stress stimulates phosphorylation of Akt in human endothelial cells. Circ Res Am Heart Assoc. 1998;83:334–41.

44. Christian F, Smith EL, Carmody RJ. The regulation of NF-κB subunits by phosphorylation. Cells. 2016;5:E12.

45. Bernardo ME, Fibbe WE. Mesenchymal stromal cells: sensors and switchers of inflammation. Cell Stem Cell. 2013;13:392–402.

## Publisher's Note